Low-threshold all-fiber 1000 nm supercontinuum source based on highly nonlinear fiber

A. Boucon, A. Fotiadi, P. Mégret, H. Maillotte, T. Sylvestre

To be published in Optics Communications 2008

Low-threshold all-fiber 1000 nm supercontinuum source based on highly non-linear fiber

Anne Boucon [a], Andrei Fotiadi [b,c], Patrice Mégret [b], Hervé Maillotte [a], Thibaut Sylvestre [a,*]

[a] Département d'Optique P.M. Duffieux, Institut FEMTO-ST, Université de Franche-Comté, CNRS UMR 6174, F-25030 Besançon Cedex, France
[b] Service d'Electromagnétisme et de Télécommunications, Faculté Polytechnique de Mons, 31 Boulevard Dolez, B-7000 Mons, Belgium
[c] Ioffe Physico-Technical Institute of Russian Academy of Sciences, 194021 Saint Petersburg, Russia

ARTICLE INFO

Article history:
Received 8 February 2008
Received in revised form 9 April 2008
Accepted 9 April 2008

Keywords:
Optical fiber
Supercontinuum generation
Non-linear optics

ABSTRACT

We present an highly efficient all-fiber compact supercontinuum source that exhibits a nearly flat spectrum from 1.1 μm to 2.1 μm. This broadband infrared optical source is made-up of a highly non-linear fiber pumped by a 1.55 μm self-Q-switched Er-Brillouin nanosecond pulsed fiber laser, which in turn is pumped by a low-power 1480 nm laser diode. In this work we highlight the great potential of highly non-linear fiber for supercontinuum generation with respect to conventional dispersion-shifted fiber by demonstrating a significant 10 dB power enhancement in the short wavelength side of the supercontinuum.

1. Introduction

In the past few years, significant research has gone into generating broadband supercontinuum (SC) light in optical fibers using compact lasers for applications ranging from components testing to optical coherence tomography [1]. An ideal SC source would provide a broadband and flat spectrum at selectable bands, while at the same time exhibiting high output spectral power stability. The use of high-peak power (kW range) Q-switched lasers for SC generation meets these requirements while keeping a low average power level. Commonly such SC sources are available mainly from the use of conventional solid-state or microchip Q-switched lasers in combination with microstructured or standard fibers with the drawback of integrating bulk laser and fiber components [2–4].

Recently, an all-fiber solution has been proposed based on a passively-Q-switched nanosecond Er-doped fiber laser [5] that allows for the achievement of an ultra-broadband SC extending from 900 nm to 1800 nm [6]. This preliminary experiment used a long standard dispersion-shifted fiber (DSF). However, significant improvement of the SC spectrum can be expected from the use of an optical fiber with more appropriate non-linear and dispersion characteristics than that of the standard DSF. Highly non-linear fiber (HNLF) has already been shown as a good candidate for operation with infrared continuous-wave SC sources [7,8] and seems to be a suitable media for operation with nanosecond pulses. Specifically, in comparison with the standard DSF, the HNLF exhibits both a stronger nonlinearity (between 5 and 15 times) and a lower dispersion slope that are key parameters for extended and flat SC generation [9]. The SC spectrum shape can precisely be controlled by the dispersion characteristics of HNLF. Moreover, the low coupling loss (0.1 dB) with standard single-mode fibers (SMF) makes HNLFs very suitable for all-fiber SC generation with respect to photonic crystal fibers [9].

In this letter, we report on a low-threshold all-fiber broadband SC source based on the use of the highly non-linear fiber in combination with sub-nanosecond self-Q-switched Er-doped fiber laser pumped by 120 mW laser diode. We show that the use of the HNLF with a zero dispersion wavelength close to the pump laser wavelength leads to efficient generation of Raman solitons and dispersive waves (DWs) in both the long and short wavelength sides of the pump, providing an enhancement of the spectral power density up to 10 dB in comparison with the SC generated in a standard DSF. The resulting SC spectrum covers the spectral window 1.1 μm–2.1 μm and has more flat profile. It is important to stress that this nanosecond IR-SC source is different from the ones demonstrated in the 1990's using high-repetition rate mode-locked fiber laser and dedicated for application to WDM-spliced telecommunication system [10,11].

2. Experimental setup

The experimental setup is schematically sketched in Fig. 1. Our device makes use of a sub-kW peak power nanosecond fiber laser with a repetition rate in the kHz range and a 500 m long HNLF for

* Corresponding author.
E-mail addresses: Andrei.Fotiadi@fpms.ac.be (A. Fotiadi), Thibaut.Sylvestre@univ-fcomte.fr (T. Sylvestre).

0030-4018/$ - see front matter © 2008 Elsevier B.V. All rights reserved.
doi:10.1016/j.optcom.2008.04.024

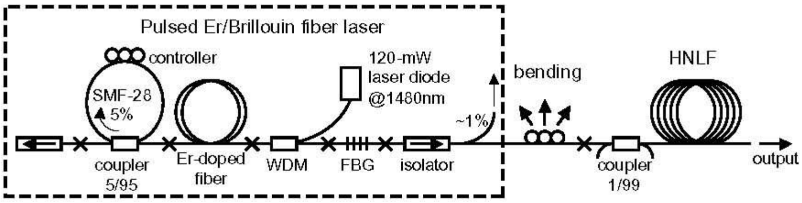

Fig. 1. Experimental setup: SMF, single-mode fiber; WDM, wavelength division multiplexing; HNLF, highly non-linear fiber.

non-linear linewidth broadening. We used the same sample of HNLF that had already demonstrated its high capability for SC generation in continuous-wave pumping regime [8].

The fiber has a non-linear coefficient of $\gamma = 11.8\ \mathrm{W^{-1}\ km^{-1}}$ and its dispersion parameters are a zero dispersion wavelength (ZDW) of 1551.4 nm and a dispersion slope of $0.032\ \mathrm{ps\ nm^{-2}\ km^{-1}}$, respectively. The cut-off wavelength for the fundamental mode is 1150 nm and its dispersion coefficients are $\beta_2 = -0.19 \times 10^{-27}\ \mathrm{s^2\ m^{-1}}$, $\beta_3 = 0.53 \times 10^{-40}\ \mathrm{s^3\ m^{-1}}$ and $\beta_4 = -0.65 \times 10^{-55}\ \mathrm{s^4\ m^{-1}}$ at 1.55 μm. The all-fiber format of the setup is maintained by direct splicing of standard telecom components.

The design of the pulsed Er/Brillouin fiber laser is nearly the same as described in Ref. [5]. The Er-doped fiber section is pumped by a 120 mW laser diode at 1480 nm through a wavelength division multiplexer. At this power level, stimulated Brillouin scattering (SBS) and Rayleigh Scattering (RS) affect the laser performance. A Brillouin ring mirror introduced into the fibre cavity through a 5/95 tap coupler provides passive generation of the nanosecond pulses (See Ref. [5] for more information about the laser dynamics). For the reported operation, pulse generation occurs with a repetition rate of 5 kHz and with an average power of 25 mW. Note that, for imaging systems like optical coherence tomography, the pulse repetition rate could be increased up to tens of kHz simply by increasing the pump power. A typical Q-switched laser pulse can be seen in Fig. 2b with a full-width at half maximum (FWHM) duration of 10 ns. The peak power was assessed to about 500 W and is subject to stochastic fluctuations around the maximum with a standard deviation of approximatively 15% [5,6]. These fluctuations are mainly due to the stochastic nature of the processes responsible for Q-switching of the laser, namely, Rayleigh scattering (RS) and stimulated Brillouin scattering (SBS). They indeed occur in a random way along the fiber and thus lead to output power instability. Note that this is turn will induce some limitations on the spectral power stability and density for the SC spectrum. Nevertheless, the repetition rate of the Q-switched laser would allow for stable long-term average measurements. The use of a fibre Bragg grating (FBG) with a 3 dB linewidth of 35 GHz (FWHM) in the laser cavity sets the laser wavelength around 1556 nm and limits the number of generated SBS Stokes components. A typical laser spectrum is shown in Fig. 2a in logarithm scale (black line) and in linear scale (grey line). The initial transmission spectrum of the FBG is also reported on Fig. 2a as a dashed line. As it can be seen, the laser emits several Brillouin Stokes lines with a full linewidth of about 0.4 nm. Note that the multi-frequency operation of the laser is beneficial for SC generation because it acts as a seed for modulation-instability-induced SC generation and helps to smooth spectral broadening [8]. By coiling the fiber on cylinders with different diameters (12 and 15 mm) we introduced irradiative losses and were able to adjust the coupling efficiency between the laser and the HNLF in order to study the SC dynamics. The output spectra were recorded with an optical spectrum analyzer (OSA) in the range 0.9–1.7 μm and with a maximum resolution of 0.06 nm. For longer wavelengths above the OSA upper limit, we used an extended spectrometer based on a 300 lines/mm diffraction grating and an InGaAs photodiode operating up to 2.6 μm. A 1% tap coupler

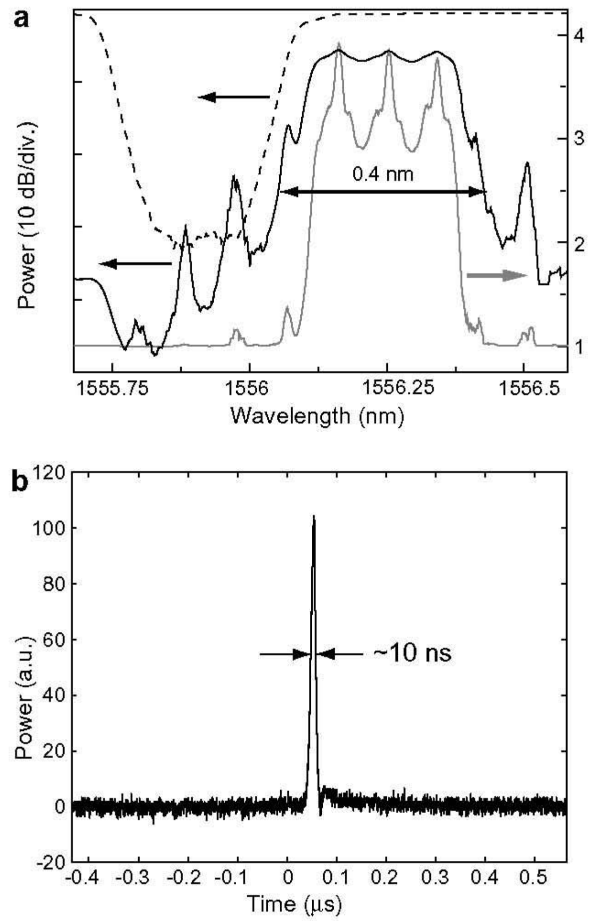

Fig. 2. (a) Typical laser output spectrum recorded with an optical spectrum analyser in logarithm scale (black line) and linear scale (grey line). Dashed line indicates the transmission spectrum of the fiber Bragg grating. (b) Oscilloscope trace of a Q-switched laser pulse.

was used for monitoring of the Er-Brillouin laser power. Finally, the full SC span was plotted by putting both spectral measurements together.

3. Results and discussion

Fig. 3 shows the SC spectrum at the fiber input and output ends at maximum launched power. The SC output power at the end of the fiber has been measured at 14 mW. We can see that most of the energy in the fundamental laser wavelength at 1556 nm is efficiently converted into the supercontinuum, therefore covering all the wavelengths between 1.1 and 1.75 μm, the latter corresponding to the OSA upper limit. The non-linear spectral broadening occurs near symmetrically on both long and short wavelength sides of the spectrum from the pump wavelength.

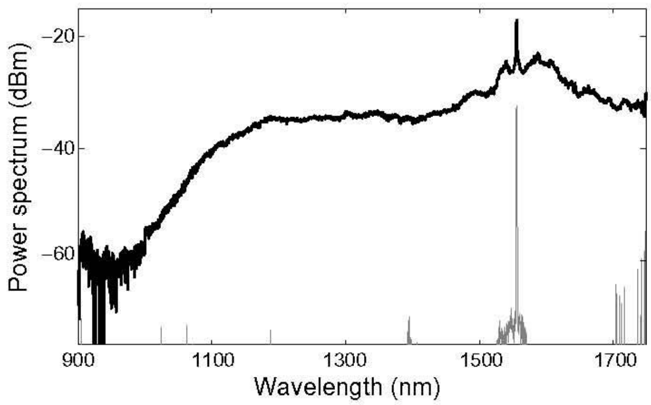

Fig. 3. Supercontinuum generation measured at maximum power (black line) and input laser spectrum (grey line).

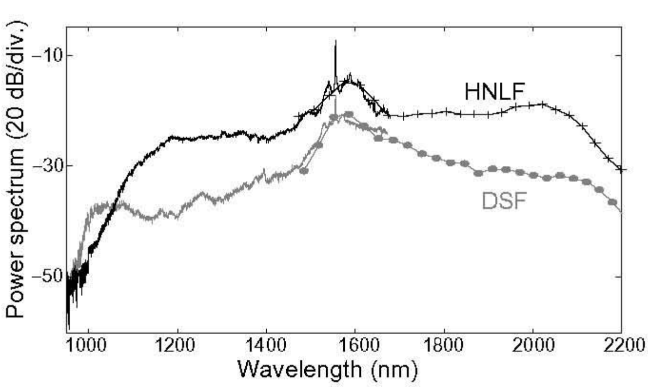

Fig. 5. Supercontinuum spectra at the output of the HNLF (black line) recorded with both OSA (solid line) and the long wavelength spectrometer (plus and rounds) and, for comparison, at the output of a DSF (grey, −10 dB offset).

Fig. 4 shows the SC build up for decreasing bending losses, or equivalently increasing coupling efficiency between the Er/Brillouin laser and the HNLF. Although femtosecond pulse SC generation involves an initial (deterministic) propagation phase of higher-order soliton evolution, SC generation in the nanosecond regime involves a significantly different scenario [1]. Specifically, the pump pulse near the ZDW undergoes spectral broadening through modulation instability (MI), which is manifested, in the frequency domain, by the generation of modulation sidebands located around the pump frequency. We can see in Fig. 4 at low-power the clear generation of two MI sidebands around the pump wavelength. These sidebands are generated because of the slight anomalous dispersion at the pump wavelength. In the time domain, MI leads to the generation of ultra-short sub-pulses train generation.

As for femtosecond pulse SC generation, these soliton-like pulses then undergo self-frequency red shift through both third-order dispersion (TOD) and stimulated Raman scattering. Simultaneously they shed energy in the form of dispersive waves at shorter wavelengths, which are enhanced by the very low dispersion slope of HNLF [8]. In Fig. 4 we can see non-solitonic DWs first around 1500 nm, and then down to 1000 nm at higher pump power. We have indeed checked that these wavelengths are in good agreement with the phase matching condition for dispersive waves emitted by soliton fission, that can be expressed at first-order as $\delta\omega = -\frac{3\beta_2}{\beta_3} \approx -6\pi c(\lambda_p - \lambda_0)$ where β_2 and β_3 are the second and third-order dispersion (TOD) coefficient, respectively. λ_p and λ_0 are the pump and the zero-dispersion wavelength [12].

Fig. 5 shows the full SC spectrum recorded using both OSA and the extended spectrometer. The solid lines correspond to the OSA graphs and plus and rounds to the measurements made with the spectrometer. First we consider the black line which corresponds to our experiment. As it can be seen, SC extends well beyond 1.75 μm and remains flat up to 2.1 μm, from which the fiber absorption increases significantly. From the latter phase-matching equation, we can infer that dispersive waves can be uniformly generated down to 1.1 μm from Raman solitons generated up to 2.1 μm. Taking into account the maximum Raman soliton frequency measured at 143 THz (or equivalently the longer SC wavelength at 2.1 μm) in Fig. 5, we obtain a theoretical DW frequency shift $\delta\nu = 152$ THz, in excellent agreement with the extension of the DWs generation towards short wavelengths. Indeed, the minimum DWs frequency is measured to 273 THz (or 1.1 μm) and corresponds to a frequency shift with respect to the pump of $\delta\nu_{\mathrm{meas}} = 130$ THz, close to the theoretically $\delta\nu_{\mathrm{th}}$. The small discrepancy can be attributed to the cut-off wavelength for the fundamental mode of the HNLF that limits the SC extension.

As a comparison, Fig. 5 also shows the SC obtained in a 200 m-long conventional DSF (grey line) [6]. Despite the fact the two fibers have different lengths because the HNLF can not be cut off, this comparison clearly highlights the advantages of the HNLF. Fig. 5 shows that a 10 dB enhancement in the SC flatness was achieved thanks to the strong nonlinearity and the low dispersion slope of the HNLF. The DSF, presenting a dispersion slope three times larger and a non-linear coefficient five times weaker than the HNLF, has less dispersive waves in the blue side of the SC spectrum.

To get better insight, we performed an additional SC generation experiment based on a concatenation of both the HNLF and the

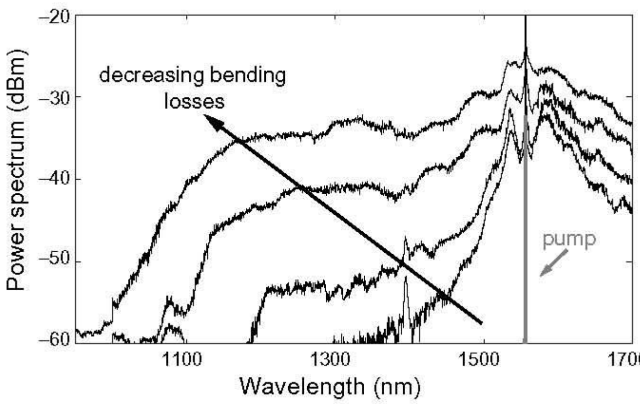

Fig. 4. Output SC spectra for decreasing bending losses between the fiber laser and the HNLF (increasing pump power).

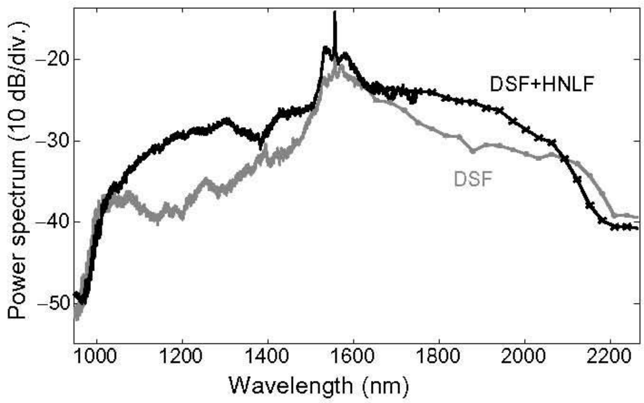

Fig. 6. Supercontinuum spectra at the output of the HNLF + DSF (black line) recorded with both OSA (solid line) and the long wavelength spectrometer (crosses and rounds) and, for comparison, at the output of the DSF (grey, same as in Fig. 5).

DSF. The results are illustrated in Fig. 6 in black line. We can see the efficient frequency conversion toward shorter wavelength, which leads to an enhancement of 10 dB between 1.1 μm and 1.5 μm. However, we can observe a decreasing spectral broadening toward longer wavelength because the HNLF's absorption increases strongly from 2.1 μm.

4. Conclusion

In conclusion, we have demonstrated a reliable 1000 nm-band nanosecond supercontinuum all-fiber source based on a highly-non-linear fiber and a passively Q-switched Erbium-doped fiber laser pumped with a 120 mW pump diode only. This simple laser source constitutes a compact and low-cost all-fiber SC source that could find direct applications in components testing or optical coherence tomography. We suggest that ultra-broadband SC can be achieved using a similar self-Q swichted Yb fiber laser at 1 μm in combination with an endlessly-single-mode microstructured fiber with a suitable dispersion.

Acknowledgements

This work was supported by Interuniversity Attraction Pole program (IAP VI 10) of the Belgian Science Policy and by the European COST Action 299. Anne Boucon thanks the Conseil Général du Doubs for funding. The authors thank Sumitomo Electric Industries (SEI) for providing the HNLF.

References

[1] J.M. Dudley, G. Genty, S. Coen, Rev. Mod. Phys. 78 (2006) 1135.
[2] A. Mussot, T. Sylvestre, L. Provino, H. Maillotte, Opt. Lett. 28 (19) (2003) 1820.
[3] W.J. Wadsworth, N. Joly, J.C. Knight, T.A. Birks, F. Biancalana, P.S.J. Russell, Opt. Exp. 12 (2) (2004) 299.
[4] P.A. Champert, V. Couderc, P. Leproux, S. Fevrier, V. Tombelaine, L. Labonte, P. Roy, C. Froehly, P. Nerin, Opt. Exp. 12 (19) (2004) 4366.
[5] A. Fotiadi, P. Mégret, M. Blondel, Opt. Lett. 29 (10) (2004) 1078.
[6] A. Fotiadi, P. Mégret, Opt. Lett. 31 (11) (2006) 1621.
[7] A. Abeeluck, C. Headley, Appl. Phys. Lett. 85 (21) (2004) 4863.
[8] T. Sylvestre, A. Vedadi, H. Maillotte, F. Vanholsbeeck, S. Coen, Opt. Lett. 31 (13) (2006) 2036.
[9] T. Nakanishi, M. Hirano, T. Okuno, M. Onishi, Silica-based highly non-linear fiber with $\gamma = 30\,\mathrm{W}^{\,1}\,\mathrm{km}^{\,1}$ and its FWM-based conversion efficiency, in: Optical Fiber Communication Conference. Available from: <http://www.opticsinfobase.org/abstract.cfm?URI=OFC-2006-OTuH7>.
[10] T. Morioka, H. Takara, S. Kawanishi, O. Kamatani, K. Takiguchi, K. Uchiyama, M. Saruwatari, H. Takahashi, M. Yamada, T. Kanamori, H. Ono, Electron. Lett. 32 (10) (1994) 906.
[11] T. Okuno, M. Onishi, M. Nishimura, IEEE Photon. Technol. Lett. 10 (1) (1998) 72.
[12] N. Akhmediev, M. Karlsson, Phys. Rev. A 51 (1995) 2602.